ELSEVIER

Ceramics International 32 (2006) 461–466

CERAMICS
INTERNATIONAL

www.elsevier.com/locate/ceramint

Effect of Y_2O_3 addition on the properties of reaction-bonded porous SiC ceramics

Shuqiang Ding[a,b,*], Sumin Zhu[a], Yuping Zeng[c], Dongliang Jiang[a]

[a] *Shanghai Institute of Ceramics, Chinese Academy of Sciences, 1295 Dingxi Road, Shanghai 200050, China*
[b] *Graduate School of the Chinese Academy of Science, Beijing 100039, China*
[c] *Synergy Materials Research Center, AIST, Nagoya 463-8687, Japan*

Received 4 February 2005; received in revised form 17 February 2005; accepted 20 March 2005

Abstract

Porous SiC ceramics were fabricated without and with Y_2O_3 addition from SiC, Al_2O_3 and graphite in air by the in situ reaction bonding process. This process is based on the oxidation of SiC and the mullitization between Al_2O_3 and oxidation-derived SiO_2. SiC particles are bonded by the mullite ($3Al_2O_3{\cdot}2SiO_2$) and SiO_2. The pores are produced by both stacking SiC particles and burning out graphite. Comparison of phase composition, microstructure, flexural strength, open porosity and pore size distribution of reaction-bonded porous SiC ceramics without and with Y_2O_3 addition was conducted. Moreover, the effect of Y_2O_3 content was investigated. Due to the enhancement of neck formation (bonding part between SiC particles) by the addition of Y_2O_3, a high strength of 27.5 MPa was achieved at an open porosity of 44.4%.

Keywords: D. SiC; D. Y_2O_3; Porous ceramics; Reaction bonding

---

1. Introduction

Due to the combination of excellent mechanical property, thermal-shock resistance and chemical stability, porous SiC ceramics have been considered as one of the ideal candidates for filters, catalytic substrates, thermal insulators, gas-burner media, and refractory materials [1–6]. Conventionally, a high temperature of generally above 2100 °C is needed for the pressureless sintering of SiC ceramics, which has limited the practical applications of porous SiC ceramics [7]. In order to realize the low-temperature fabrication of porous SiC ceramics, oxides are usually added into the starting materials to bond SiC particles [8–10]. She and Deng developed an oxidation-bonding technique for the fabrication of porous SiC ceramics at low temperatures [11]. In their work, SiC compacts were heated in air and due to the surface oxidation, SiC particles were bonded by the oxidation-derived SiO_2 glass. Recently, we have fabricated porous SiC ceramics from SiC, Al_2O_3 and graphite in air by the in situ reaction bonding process [12]. This process is based on the oxidation of SiC and the mullitization between Al_2O_3 and the oxidation-derived SiO_2. SiC particles are bonded by mullite ($3Al_2O_3{\cdot}2SiO_2$) and SiO_2. The pores are produced by stacking SiC particles and burnout of graphite. Since the thermal expansion coefficient of mullite (5.3×10^{-6}/K at 273–1273 K) approximates to that of SiC (4.7×10^{-6}/K at 273–1273 K) and mullite possesses superior mechanical property at both room and elevated temperatures, as-fabricated porous SiC ceramics are expected to exhibit better properties. In order to lower the sintering temperature of porous SiC ceramics, Y_2O_3 has been chosen as sintering additive.

The objective of present work is to investigate the effect of Y_2O_3 on the fabrication of porous SiC ceramics. Comparison of phase composition, microstructure, flexural strength, open porosity and pore size distribution of porous SiC ceramics without and with Y_2O_3 addition have been conducted. Moreover, the effect of Y_2O_3 content on the properties of porous SiC ceramics has been investigated.

---

[*] Corresponding author. Tel.: +86 21 52415232; fax: +86 21 52413903.
E-mail address: sqding@mail.sic.ac.cn (S. Ding).

0272-8842/$30.00 © 2005 Elsevier Ltd and Techna Group S.r.l. All rights reserved.
doi:10.1016/j.ceramint.2005.03.024

2. Experimental procedure

Commercially available α-SiC (99.4% purity, average particle size of 20.0 μm, Weifang Kaihua Silicon Carbide Micro-powder Co. Ltd., Weifang, China) and α-Al_2O_3 (95% crystalline phase, 0.6 μm, Wusong Chemical Fertilizer Factory, Shanghai, China) were used as the starting materials. To obtain porous SiC ceramics with different porosities, graphite powder (99.9% purity, 20.0 μm, Qingdao HuaTai Lubricant Sealling Science and Technology Co. Ltd., Qingdao, China) was employed as the pore-forming agent. Moreover, Y_2O_3 (99.9% purity, 5.0 μm, Shanghai Yuelong Non-ferrous Metal Co. Ltd., Shanghai, China) was used as sintering additive to improve the mechanical properties and lower the sintering temperature. The weight ratio of SiC, Al_2O_3 and graphite is 5:3:2. The powder mixtures of SiC, Al_2O_3 and C without and with Y_2O_3 were mixed at certain ratios and ball-milled in methanol for 24 h to increase the homogeneity. After drying in an oven and being sieved through a 75-mesh screen, the powders were bidirectionally pressed into the rectangular specimens of 4.5 mm × 10.0 mm × 50.0 mm under a 50 MPa pressure using a stainless steel die. The specimens were heated in air in a box furnace.

Weights of all samples were measured before and after sintering to estimate the oxidation degree of SiC particles. Open porosity was determined by the Archimedes method with distilled water as liquid medium. Pore size distribution was obtained using mercury porosimetry. Flexural strength was measured by a three-point bending test with a support distance of 30 mm and a cross-head speed of 0.5 mm/min on specimens of 3.0 mm × 4.0 mm × 36.0 mm. Four specimens were tested to obtain the average strength. Phase analysis was conducted by X-ray diffraction (XRD). Microstructures and morphology were observed by scanning electron microscopy (SEM). Moreover, the oxidation behavior of graphite powders in air was evaluated by thermogravimetry (TG) analysis.

3. Results and discussion

As is shown in Fig. 1, graphite oxidation begins at ~600 °C and completes at ~850 °C. Thus, heating rate must be kept slow between 600 °C and 850 °C because a high heating rate may result in acute release of CO_2 during burning of graphite and it will cause the collapse of green bodies. SiC particles begin to oxidize at ~750 °C [11]. This means that the network structure of green bodies can be stabilized by partly residual graphite before 850 °C and by oxidation-derived SiO_2 after 850 °C, which ensures green bodies against destruction.

Oxidation rate of SiC in air is diffusion-controlled and follows a parabolic law [13,14]. According to the parabolic law, the square of SiC oxidation degree versus time is a linear relation when SiC is oxidized in air at certain a temperature. The increase of heating temperature and holding time may promote the oxidation of SiC. The products of SiC oxidation are amorphous silica or cristobalite, depending on the temperature. It is shown in Fig. 2 that amorphous silica begins to crystallize into cristoballite after 1100 °C. The transformation of amorphous silica to cristoballite strengthens the bonding part between SiC particles.

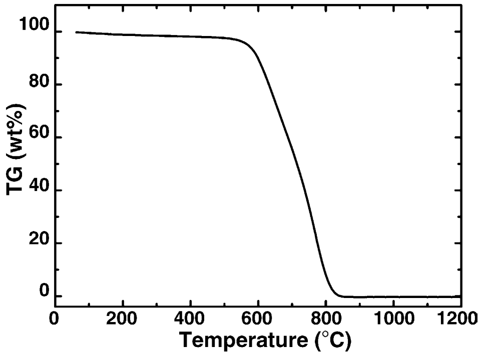

Fig. 1. TG curve of the graphite heated in air at a rate of 5 °C/min.

Fig. 3 shows the XRD patterns of the specimens without and with 1.5 wt.% Y_2O_3 addition, respectively, which were sintered at different temperatures. For the specimens without Y_2O_3, mullitization occurs at 1400 °C due to the reaction between Al_2O_3 and oxidation-derived SiO_2, as shown in Fig. 3a. It is noteworthy that the mullitization is not completed, with the evidence that Al_2O_3 peaks exist in XRD patterns and that mullitization degree increases at higher sintering temperatures. Obvious peaks of mullite do not appear in the XRD patterns until 1450 °C. At 1500 °C, extensive mullitization occurs. As the temperature is further increased to 1550 °C, mullitization reaction is nearly completed with only a trace of unreacted Al_2O_3. On the other hand, the content of cristobalite increases acutely when sintering temperature is elevated. This should be attributed to the fact that the higher temperature accelerates the diffusion of oxygen through SiO_2 film on the surface of SiC particles. While 1.5 wt.% Y_2O_3 was added, the temperature of mullitization drops by nearly 100 °C.

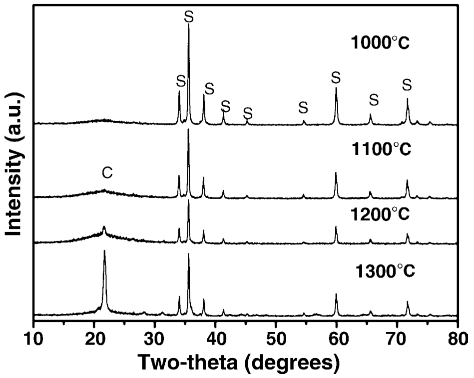

Fig. 2. XRD patterns of SiC oxidation at the indicated temperatures (C is cristobalite and S is silicon carbide).

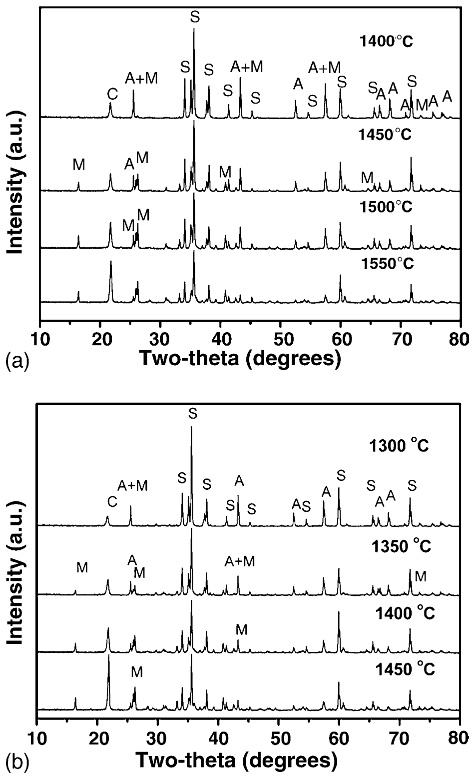

Fig. 3. XRD patterns of porous SiC ceramics (a) without Y_2O_3 addition and (b) with 1.5 wt.% Y_2O_3, sintered at the indicated temperatures for 4 h (A is alumina, C is cristobalite, M is mullite and S is silicon carbide).

At 1450 °C, mullitization reaction is almost completed and a considerable amount of cristobalite has been formed (in Fig. 3b). As a result, SiC particles are bonded by amorphous silica, cristobalite and mullite. Thus, the sintering of porous ceramics is realized by a variety of in situ reactions on the surface of SiC particles:

$$SiC + 2O_2 \rightarrow SiO_2\,(\text{amorphous}) + CO_2 \qquad (1)$$

$$\text{Amorphous}\, SiO_2 \rightarrow \text{cristobalite} \qquad (2)$$

$$3Al_2O_3 + 2SiO_2 \rightarrow 3Al_2O_3{\cdot}2SiO_2\,(\text{mullite}) \qquad (3)$$

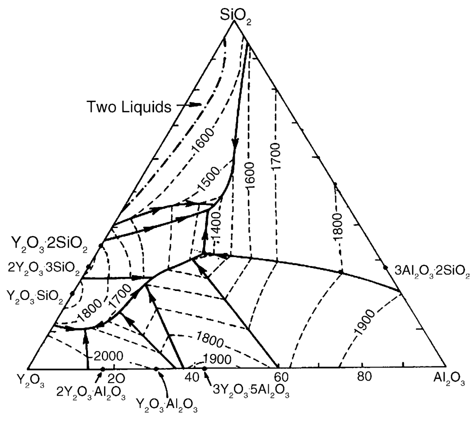

Fig. 4. Al_2O_3–Y_2O_3–SiO_2 phase diagram proposed by I.A. Bondar and F.Va. Galakhov [18].

Since the porous ceramics have been fabricated by the in situ reaction process, the homogeneous properties in physics and chemistry would be expected [15].

The decrease of mullitization temperature after Y_2O_3 addition can be explained by the mechanism of mullite formation. Based on the previous works [16,17], mullitization is controlled by the solution-precipitation mechanism. According to this mechanism, the reaction between SiO_2 and Al_2O_3 produces a metastable eutectic liquid to form a transitory aluminosilicate glass and then, alumina is dissolved into the aluminosilicate glass to precipitate mullite. When Y_2O_3 exists, Y_2O_3–SiO_2–Al_2O_3 can form the metastable eutectic liquid at lower temperature than SiO_2–Al_2O_3. This can be seen from the phase diagram of Al_2O_3–Y_2O_3–SiO_2 (Fig. 4). Thus, the addition of Y_2O_3 results in the decrease of mullitization temperature.

Typical microstructure of porous SiC ceramics without Y_2O_3 addition is shown in Fig. 5a, which exhibits a loose

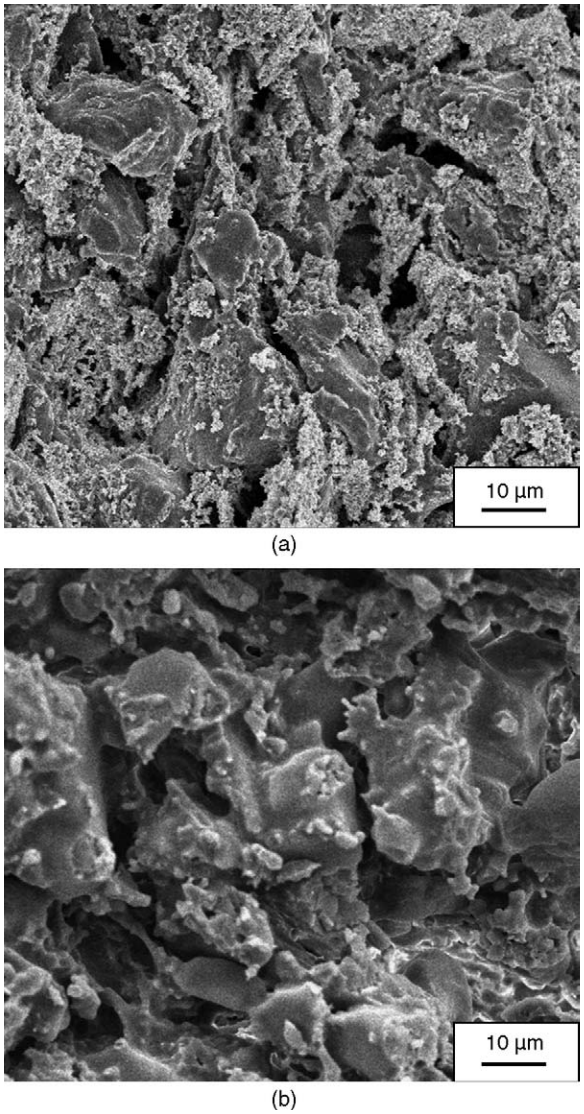

Fig. 5. SEM micrograph of porous SiC ceramics (a) without Y_2O_3 addition and (b) with 1.5 wt.% Y_2O_3, sintered at 1450 °C for 4 h.

structure with obvious connected pores. There are many floccules on the surface of SiC particles. It can be deduced according to the results of the above XRD patterns that these floccules are mainly amorphous silica and unreacted alumina. Though mullitization occurs in porous ceramics, the densification has not been taken on due to the mullitization prior to the densification [19]. This ensures a loose structure with plenty of pores. In porous ceramics, the pores are derived from stacking SiC particles and burnout of graphite. Since the SiC and graphite of 20 μm were used as starting materials, the diameter of pores from graphite burnout should be larger than the one from stacking SiC particles. Fig. 5b shows the fractural morphology of porous SiC ceramics with 1.5 wt.% Y_2O_3 addition. Compared with the specimen without Y_2O_3 addition, the fracture surface is clearer and more compacted with smaller pores. This could be attributed to the fact that the addition of Y_2O_3 promotes the formation of metastable eutectic liquid and reduces its viscosity so that the crystallization and mullitization become easier. Consequently, more cristobalite is formed and less unreacted Al_2O_3 is remained. In addition, the low viscosity of eutectic liquid will flow into the pore channels so that some small pores are filled up and the diameter of large pores decreases.

Fig. 6 shows the effects of Y_2O_3 addition on SiC oxidation, flexural strength and open porosity of the porous ceramics sintered at different temperatures. As can be seen in Fig. 6a, both the increase of sintering temperature and the addition of Y_2O_3 promote the oxidation of SiC. Oxygen diffusion through silica film on the surface of SiC becomes faster at higher temperature and then the oxidation of SiC is speeded up. On the other hand, Y_2O_3 addition leads to the formation of lower viscosity of Y–Al–Si–O glass phase [20], which improves the diffusion rate of oxygen in it and accelerates the oxidation of SiC. Based on the above discussion, higher sintering temperature results in more oxidation-derived silica and also promotes the formation of cristobalite and mullite. More silica and mullite can strengthen the bonding of SiC particles. Thus, Y_2O_3 addition enhances the oxidation and mullitzation and further improves the strength. However, when 1.5 wt.% Y_2O_3 is added, too high sintering temperature results in excessive Y–Al–Si–O glass phase and reduces the strength instead (in Fig. 6b). Fig. 6c shows that open porosity decreases with the sintering temperature and open porosity of porous ceramics with 1.5 wt.% addition is larger than the one without Y_2O_3 addition, which is in agreement with the microstructure observations (Fig. 5). When sintering temperature increases, more silica are formed and more amorphous silica is crystallized to cristobalite. The formation of amorphous silica and cristobalite is accompanied with acute volume expansion but the results of the experiments show that the dimension of all the specimens before and after sintering is almost invariable. Thus, the expanded volume has been extended into the voids among SiC particle, which leads to the decrease of open porosity.

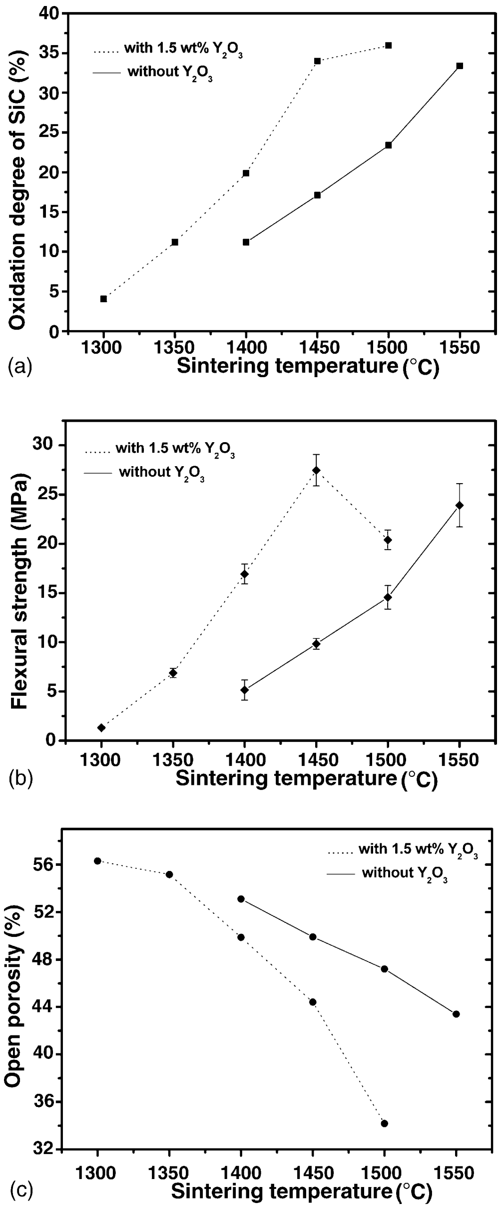

Fig. 6. Effects of sintering temperature on (a) oxidation degree of SiC, (b) porosity and (c) flexural strength of porous SiC ceramics without and with Y_2O_3 addition, sintered for 4 h.

Further characterization of the pore size distribution in porous SiC ceramics was performed by mercury porosimetry. As shown in Fig. 7, the curves are dual-peaked, the pore size distribution is narrow and the size of all pores is smaller than 10.0 μm. Since the size of the pores from stacking SiC particles is smaller than that from burnout of graphite, the former peak in the curves should correspond to the pores caused by stacking SiC particles and the latter corresponds to the pores from burnout of graphite. It is interesting that when Y_2O_3 is added, the size of the pores by stacking SiC particles increases while the size of the pores from burnout of graphite decreases. It can be understood from the fact that the lowly viscous Y–Al–Si–O glass

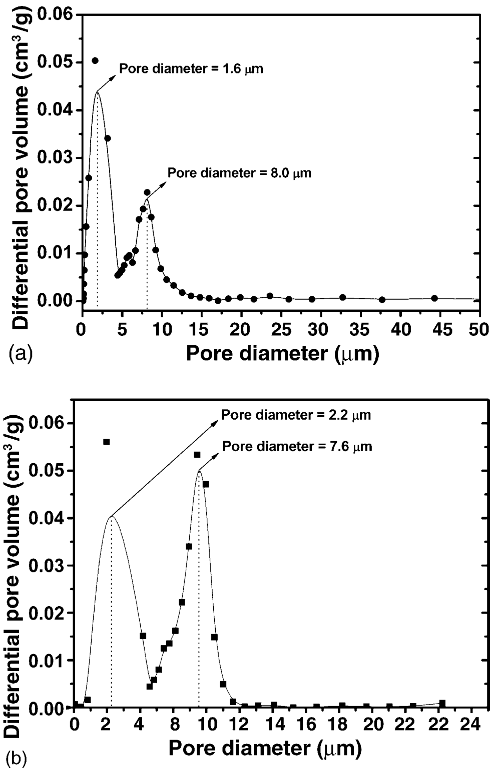

Fig. 7. Pore size distribution in porous SiC ceramics (a) without Y_2O_3 addition and (b) with 1.5 wt.% Y_2O_3, sintered at 1450 °C for 4 h.

formed after Y_2O_3 addition will flow into some small pores from stacking SiC particles and fill them up so that only larger pores are left and the average diameter of the pores from stacking SiC particles increases. However, the large pores from the burnout of graphite can not be filled up but only be thinned by Y–Al–Si–O glass.

Since Y–Al–Si–O glass has great effect on the properties of porous SiC ceramics and the formation of Y–Al–Si–O glass is closely related with the Y_2O_3 content, Y_2O_3 with different contents has been added into the starting materials. Effects of Y_2O_3 content on SiC oxidation, flexural strength and open porosity of porous SiC ceramics are shown in Table 1. It can be seen that an increasing Y_2O_3 content promotes the oxidation of SiC and improves the strength of porous SiC ceramics. However, the flexural strength first increases and then decreases with Y_2O_3 content. When 1.5 wt.% Y_2O_3 is added, the maximal strength of 27.47 MPa is achieved at an open porosity of 44.4%. This should be attributed to the fact that the increase of Y_2O_3 content results in more Y–Al–Si–O glass, mullite and cristobalite (Fig. 8). Mullite and cristobalite can enhance the strength of porous ceramics, but the strength is impaired when excessive Y–Al–Si–O glass exists in the porous ceramics because this glass is fragile and many closed pores are covered in it. As a result, too much Y_2O_3 addition is disadvantageous to the strength of porous SiC ceramics.

Table 1
Y_2O_3 dependence of SiC oxidation degree, porosity and flexural strength of porous SiC ceramics sintered at 1450 °C for 4 h

Y_2O_3 content (wt.%)	SiC oxidation degree (%)	Open porosity (%)	Flexural strength (MPa)
0	17.1	49.9	9.8 ± 0.6
0.5	25.1	48.3	18.6 ± 1.3
1.5	34.0	44.4	27.5 ± 1.7
3.0	44.6	42.0	25.8 ± 1.7
4.5	53.9	41.8	24.1 ± 2.9

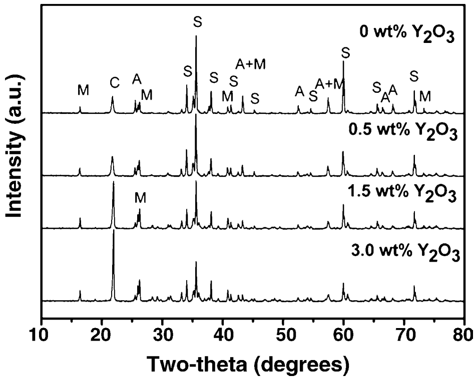

Fig. 8. XRD patterns of porous SiC ceramics with different Y_2O_3 contents, sintered at 1450 °C for 4 h (A is alumina, C is cristobalite, M is mullite and S is silicon carbide).

4. Conclusions

SiC porous ceramics were fabricated without and with Y_2O_3 addition from SiC, Al_2O_3 and graphite in air by the in situ reaction bonding process. The temperature of mullite formation was reduced by nearly 100 °C and more silica was formed when 1.5 wt.% Y_2O_3 was added. Y_2O_3 could react with Al_2O_3 and oxidation-derived SiO_2 to form the lowly viscous Y–Al–Si–O glass which speeds up the oxidation of SiC and the formation of mullite, improves the strength and diminishes the open porosity. Moreover, it was found that the addition of Y_2O_3 enlarged the average size of the pores from stacking SiC particles but diminished the average size of the pores from burnout of graphite. When Y_2O_3 content was higher, SiC oxidation degree increased and open porosity decreased. However, the flexural strength of porous SiC ceramics first increased and then decreased with the Y_2O_3 content. When Y_2O_3 content was 1.5 wt.%, the maximal strength of 27.5 MPa was achieved at an open porosity of 44.4%.

Acknowledgements

The authors thank for the financial support from the “Plan of Outstanding Talents” of Chinese Academy of Sciences. The comments of the reviewers are greatly appreciated.

References

[1] S. Zhu, S. Ding, H. Xi, R. Wang, Low-temperature fabrication of porous SiC ceramics by preceramic polymer reaction bonding, Mater. Lett. 59 (2005) 595–597.

[2] J.W. Brockmayer, J.E. Dore, US Patent 4 885 263, 5 December 1989.

[3] I. Nettleship, Applications of porous ceramics, Key Eng. Mater. 122–124 (1996) 305–324.

[4] D.J. Green, P. Colombo, Cellular ceramics: intriguing structures, novel properties, and innovative applications, MRS Bull. 28 (2003) 296–300.

[5] P. Greil, Advanced engineering ceramics, Adv. Mater. 14 (2002) 709–716.

[6] L.J. Gibson, Cellular solids, MRS Bull. 28 (2003) 270–271.

[7] L.S. Sigl, Core/rim structure of liquid-phase-sintered silicon carbide, J. Am. Ceram. Soc. 76 (1993) 773–776.

[8] Y. Lin, C. Tsang, Fabrication of mullite/SiC and mullite/zirconia/SiC composites by 'dual' in-situ reaction syntheses, Mater. Sci. Eng. A 344 (2003) 168–174.

[9] X. Zhu, D. Jiang, S. Tan, Reaction bonding of open cell SiC–Al_2O_3 composites, Mater. Res. Bull. 36 (2001) 2003–2015.

[10] K.P. Gadkaree, US Patent 6,736,875 B2, 18 May 2004.

[11] J. She, Z. Deng, Oxidation bonding of porous silicon carbide ceramics, J. Mater. Sci. 37 (2002) 3615–3622.

[12] S. Ding, S. Zhu, D. Jiang, Fabrication and properties of silica-mullite bonded silicon carbide porous ceramics (submitted for publication).

[13] P.J. Jorgensen, M.E. Wadsworth, I.B. Cutler, Oxidation of silicon carbide, J. Am. Ceram. Soc. 12 (1959) 613–616.

[14] G. Ervin, Oxidation behavior of silicon carbide, J. Am. Ceram. Soc. 41 (1958) 347–352.

[15] G.J. Zhang, T. Ohji, In situ reaction of silicon carbide-boron nitride composites, J. Am. Ceram. Soc. 84 (2001) 1475–1479.

[16] R.F. Davis, J.A. Pask, Diffusion and reaction studies in the system Al_2O_3–SiO_2, J. Am. Ceram. Soc. 55 (1972) 525–531.

[17] K. Liu, G. Thomas, A. Cabalerok, J.S. Moya, S.D. Aza, Mullite formation in kaolinite-α-alumina, Acta Metall. Mater. 42 (1994) 489–495.

[18] M.K. Reser, Phase Diagrams for Ceramists 1969 Supplement, The American Ceramic Society, USA, 1969, pp. 165.

[19] Y. Nurishi, J.A. Pask, Sintering of α-Al_2O_3 amorphous silica compacts, Ceram. Int. 8 (1982) 57–59.

[20] J. She, P. mechnich, Reaction-bonding behavior of mullite ceramics with Y_2O_3 addition, J. Eur. Ceram. Soc. 22 (2002) 323–328.